Electromagnetics, 25:425–435, 2005

ISSN: 0272-6343 print/1532-527X online
DOI: 10.1080/02726340590957416

Taylor & Francis
Taylor & Francis Group

Superlattice Properties of Helical Nanostructures in a Transverse Electric Field

O. V. KIBIS
S. V. MALEVANNYY

Department of Applied and Theoretical Physics
Novosibirsk State Technical University
Novosibirsk, Russia

L. HUGGETT
D. G. W. PARFITT
M. E. PORTNOI

School of Physics
University of Exeter
Exeter, United Kingdom

A charge carrier confined in a quasi-one-dimensional helical nanostructure in the presence of an electric field normal to the axis of the helix is subjected to a periodic potential proportional to the strength of the field and the helix radius. As a result, the behavior of this carrier is similar to that in a semiconductor superlattice with parameters controlled by the applied field. This behavior includes Bragg scattering of the charge carrier by a periodic potential, which results in an energy gap opening at the edge of the superlattice Brillouin zone. A certain type of carbon nanotube is shown to possess similar superlattice properties. Modification of the band structure is found to be significant for experimentally attainable electric fields, which raises the possibility of applying this effect to novel nanoelectronic devices.

Keywords superlattice, helical nanostructure, carbon nanotube

Introduction

One of the main elements of modern nanoelectronics is the superlattice: an artificial solid-state structure with potential variations that have a period of several tenths of the interatomic separation (see, e.g., Ivchenko & Pikus, 1997). Bragg diffraction of electronic waves on such a superperiod results in significant modification of the electronic energy spectrum (in particular, the appearance of energy gaps). This allows the creation of nanoelectronic devices with specific characteristics. In existing technological processes these

Received 18 November 2004; accepted 17 January 2005.
This work was supported by the Royal Society, INTAS, the Russian Foundation for Basic Research, and the "Russian Universities" program.
Address correspondence to M. E. Portnoi, School of Physics, University of Exeter, Stocker Road, Exeter EX4 4QL, United Kingdom. E-mail: m.e.portnoi@exeter.ac.uk

superlattices are based on multilayer semiconductor heterostructures. The parameters of the periodic potential are therefore defined by the growth conditions and cannot be manipulated subsequently. Hence, it is highly desirable to develop a new kind of superlattice in which the periodic potential parameters may be altered by an applied electric field. This will provide an opportunity for creating a new class of nanoelectronic devices with controlled properties. In this paper we present a theoretical analysis of a novel type of superlattice with variable parameters, based on different helical nanostructures.

Semiconductor Nanohelices in a Transverse Electric Field

It has recently become possible to fabricate semiconductor nanohelices based on InGaAs/GaAs (Prinz et al., 2000) and Si/SiGe (Prinz et al., 2001). Let us consider such a nanohelix as a one-dimensional conductor with total length L, in the shape of a helix with radius R and pitch P, in an external electric field of magnitude E normal to the axis of the helix. The potential energy of an electron in such a helix is given by

$$U(s) = eER\cos(2\pi s/l_0), \tag{1}$$

where e is the electron charge, s is the electron coordinate along the one-dimensional conductor, and $l_0 = \sqrt{4\pi^2R^2 + P^2}$ is the length of a single coil of the helix. Evidently, the potential energy (1) is periodic with respect to the electron coordinate s, with period l_0, which is significantly larger than the interatomic distance. As a result, the nanohelix acquires typical superlattice properties. In the framework of the effective mass model, the energy spectrum ε_E of an electron in a nanohelix in a transverse electric field is obtained from the Schrödinger equation:

$$-\frac{\hbar^2}{2m}\frac{d^2}{ds^2}\psi_E + U(s)\psi_E = \varepsilon_E\psi_E, \tag{2}$$

where m is the effective mass of the electron. The solutions ψ_E of Eq. (2) are known to be Mathieu functions (Gradshteyn & Ryzhik, 2000). However, despite the exact solutions being known, it is impossible to write the energy spectrum ε_E in analytic form as a function of the electron wavenumber k along the helical line. Since the dispersion $\varepsilon_E(k)$ determines the main electrophysical parameters of a superlattice, it is necessary to find it explicitly. We will therefore use an approximate method of solving Eq. (2). Let us search for a wavefunction ψ_E as a superposition of plane waves $\psi_0(k) = \sqrt{1/L}\exp(iks)$, which are the eigenfunctions of the electron in the absence of the external electric field:

$$\psi_E = \sum_k b_k\psi_0(k). \tag{3}$$

The matrix element of the potential energy (1) connecting unperturbed electron states with wavenumbers k and k' is then

$$\langle\psi_0(k')|U(s)|\psi_0(k)\rangle = \pi eER\left[\delta(kL - k'L + gL) + \delta(kL - k'L - gL)\right], \tag{4}$$

where $g = 2\pi/l_0$ is the width of the first superlattice Brillouin zone. Substituting the plane wave expansion (3) into the Schrödinger equation (2), and taking into account Eq. (4), we obtain the system of linear algebraic equations

$$\left[\varepsilon_0(k) - \varepsilon_E(k)\right]b_k + U_E\left(b_{k+g} + b_{k-g}\right) = 0, \tag{5}$$

where

$$\varepsilon_0(k) = \frac{\hbar^2 k^2}{2m} \tag{6}$$

is the unperturbed energy of an electron in a nanohelix in the absence of an external electric field, and $U_E = eER/2$ is the characteristic energy of interaction of the electron with the electric field.

The matrix element (4) is nonzero only for electron states with wavenumbers differing by g. Therefore, for weak enough electric fields, satisfying the condition $U_E/\varepsilon_0(g) \ll 1$, when solving the system of equations (5) it is sufficient to take into account the admixture of only the two states closest in energy, neglecting the contribution of all other states separated by an energy exceeding U_E. In this approximation the system of equations (5), which defines the electron energy spectrum $\varepsilon_E(k)$, is reduced to just two equations, from which the electron energy can be written in the extended Brillouin zone scheme as

$$\varepsilon_E(k) = \begin{cases} \frac{1}{2}[\varepsilon_0(k) + \varepsilon_0(|k| - g)] - \frac{1}{2}\sqrt{[\varepsilon_0(k) - \varepsilon_0(|k| - g)]^2 + 4U_E^2}, & |k| \le g/2 \\ \frac{1}{2}[\varepsilon_0(k) + \varepsilon_0(|k| - g)] + \frac{1}{2}\sqrt{[\varepsilon_0(k) - \varepsilon_0(|k| - g)]^2 + 4U_E^2}, & |k| \ge g/2 \end{cases} \tag{7}$$

The energy spectrum given by Eq. (7) is plotted in Figure 1. It follows from Eq. (7) that the transverse electric field results in the opening of a gap in the nanohelix energy spectrum at the boundary of the first Brillouin zone at $k = \pm g/2$. The middle of this gap lies at the energy $\varepsilon_0(g/2)$ above the bottom of the unperturbed conduction band; the size of the gap is linearly dependent on the field strength E and is equal to

$$\Delta\varepsilon = 2U_E = eER. \tag{8}$$

It should be noted that the energy gaps at the boundaries of the other Brillouin zones depend on higher powers of the electric field E, and contain a small parameter $U_E/\varepsilon_0(g) \ll 1$. These gaps are neglected in the approximate expression (7).

Equations (7) and (8) clearly show that a nanohelix in a transverse electric field represents a superlattice with the parameters controlled by the applied field.

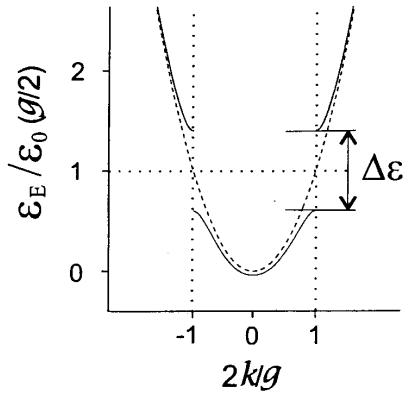

Figure 1. Electron energy spectrum of a nanohelix in the presence of a transverse electric field $E = 0.2\varepsilon_0(g)/(eR)$ (solid lines) and without the electric field (dashed line).

Carbon Nanotubes as Superlattices

Carbon nanotubes (CNTs) are cylindrical molecules with nanometre diameter and micrometre length. Since the discovery of CNTs just over a decade ago (Iijima, 1991), their unique electronic and structural properties have aroused great excitement in the scientific community and promise a broad range of applications. Significant theoretical effort has been applied to develop refined models of the electronic structure of carbon nanotubes, as well as their optical and transport properties, although even a simple tight-binding model (see Saito, Dresselhaus, & Dresselhaus, 1998) yielding analytic solutions is sufficient to elucidate key nanotube features (e.g., whether a CNT of given structure will exhibit metallic or semiconducting properties). In what follows we apply such a model to a particular type of single-wall CNT, a so-called $(n, 1)$ nanotube. We show that for such a CNT the electron motion corresponds to a de Broglie wave propagating along a helical line. The theoretical treatment of this type of CNT in an electric field perpendicular to the nanotube axis (transverse electric field) can be reduced to a one-dimensional superlattice problem (Kibis, Parfitt, & Portnoi, 2005). Such superlattice behavior of current-carrying electrons suggests the application of CNTs to the development of novel carbon nanotube-based devices.

A single-wall carbon nanotube may be considered as a single graphite sheet rolled into a cylinder. The electronic energy spectrum of the CNT is therefore intimately related to the energy spectrum $\varepsilon_{g2D}(\mathbf{k})$ of a two-dimensional (2D) graphite sheet, which can be written in the tight-binding approximation as (Saito, Dresselhaus, & Dresselhaus, 1998)

$$\varepsilon_{g2D}(\mathbf{k}) = \pm\gamma_0 \left| \exp\left(\frac{ik_x a}{\sqrt{3}}\right) + 2\exp\left(-\frac{ik_x a}{2\sqrt{3}}\right)\cos\left(\frac{k_y a}{2}\right)\right|, \tag{9}$$

where k_x and k_y are the electron wave vector components in the graphite sheet plane along the x and y axes, respectively (see Figure 2). In the energy spectrum (9), the plus and minus signs correspond to the conduction and valence bands, respectively; $\gamma_0 \approx 3$ eV is the transfer integral between π-orbitals of neighboring carbon atoms, and the lattice constant $a = |\mathbf{a}_1| = |\mathbf{a}_2| = \sqrt{3} \times a_{\text{C-C}} = 2.46$ Å, where $\mathbf{a}_1$ and $\mathbf{a}_2$ are the 2D basis vectors and $a_{\text{C-C}} = 1.42$ Å is the interatomic distance in graphite. The way in which the 2D graphite sheet is rolled up to form the CNT can be described by two vectors: the translation vector $\mathbf{T}$ and the chiral vector $\mathbf{C}_h$ (see Figure 2). The chiral vector $\mathbf{C}_h$ can be expressed in terms of the 2D basis vectors of the unrolled graphite sheet as $\mathbf{C}_h = n\mathbf{a}_1 + m\mathbf{a}_2$, where the pair of integers (n, m) is used as a standard notation (Saito, Dresselhaus, & Dresselhaus, 1998) for a CNT of given crystal structure. To obtain the electronic energy spectrum of the (n, m) CNT, we begin by expressing the wave vector $\mathbf{k}$ in terms of components along $\mathbf{T}$ and $\mathbf{C}_h$ as $\mathbf{k} = k_\parallel \mathbf{T}/T + k_\perp \mathbf{C}_h/C_h$, where $k_\parallel$ and $k_\perp$ are subject to the following constraints: $-\pi/T < k_\parallel \leq \pi/T$ and $k_\perp = 2\pi l/C_h$ $(l = 0, 1, 2, \ldots, N-1)$. The integer l represents the electron angular momentum along the nanotube axis and

$$N = \frac{2(n^2 + m^2 + nm)}{d_R}, \tag{10}$$

is the number of elementary atomic cells consisting of two carbon atoms (A, B) per area $|\mathbf{C}_h \times \mathbf{T}|$. The number d_R appearing in Eq. (10) is the greatest common divisor of the two integers $(2n + m, 2m + n)$. The lengths of the chiral vector and translation vector are given by $C_h = a\sqrt{n^2 + m^2 + nm}$ and $T = \sqrt{3}C_h/d_R$, respectively.

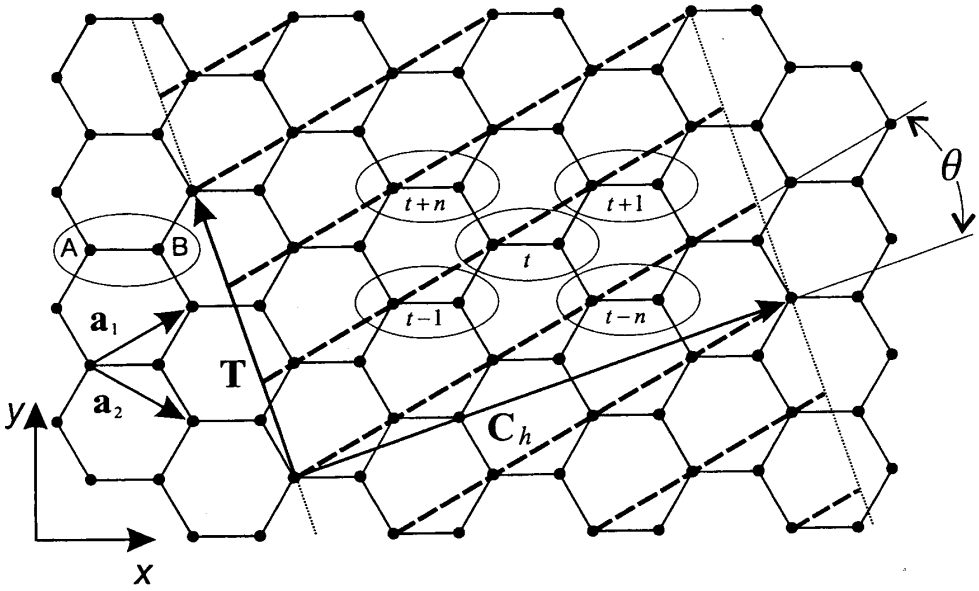

Figure 2. The unrolled graphite sheet. By connecting the head and tail of the chiral vector $\mathbf{C}_h$ we can construct, for example, a (4, 1) carbon nanotube. The dashed lines will then form a helical line on the nanotube wall.

The energy spectrum of an (n, m) CNT can be obtained by expressing k_x and k_y in terms of $k_\parallel$ and $k_\perp$, and substituting them in Eq. (9), thus yielding

$$\varepsilon = \pm\gamma_0 \left| \exp\left[\frac{i\sqrt{3}a}{2} \left(k_\parallel \cos\theta - k_\perp \sin\theta \right) \right] + 2\cos\left(\frac{k_s a}{2} \right) \right|, \tag{11}$$

where we have introduced the new parameter $k_s = k_\perp \cos\theta + k_\parallel \sin\theta$, and the chiral angle θ ($|\theta| \leq \pi/6$) shown in Figure 2. Taking into account that

$$\cos\theta = \frac{2n+m}{2\sqrt{n^2+m^2+nm}}, \quad \sin\theta = \frac{\sqrt{3}m}{2\sqrt{n^2+m^2+nm}}, \tag{12}$$

we have, for $m \neq 0$, the equation

$$\sqrt{3}(k_\parallel \cos\theta - k_\perp \sin\theta)a = [(2n+m)k_s a - 2k_\perp C_h]/m. \tag{13}$$

Substituting Eqs. (12) and (13) into Eq. (11) we obtain

$$\varepsilon = \pm\gamma_0 \left| \exp\left[i \left(\frac{2n+m}{2m} k_s a - \frac{k_\perp C_h}{m} \right) \right] + 2\cos\left(\frac{k_s a}{2} \right) \right|, \tag{14}$$

which, together with the constraint $k_\perp = 2\pi l / C_h$, yields an electron energy spectrum of the form

$$\varepsilon = \pm\gamma_0 \left[1 + 4\cos\left(\frac{k_s a}{2} \right) \cos\left(\frac{2n+m}{2m} k_s a - \frac{2\pi l}{m} \right) + 4\cos^2\left(\frac{k_s a}{2} \right) \right]^{1/2}. \tag{15}$$

For $m = 1$, Eq. (15) becomes independent of l, and we obtain the electron energy spectrum of a $(n, 1)$ CNT in the form

$$\varepsilon_j(k_s) = (-1)^j \gamma_0 \left[1 + 8\cos\left(\frac{n+1}{2}k_s a\right)\cos\left(\frac{nk_s a}{2}\right)\cos\left(\frac{k_s a}{2}\right)\right]^{1/2}, \tag{16}$$

where $j = 1, 2$ correspond to the valence and conduction bands, respectively. It should be noted that the spectrum (16) depends on the parameter k_s alone, in contrast to the general case of an (n, m) CNT, for which the electron energy spectrum depends on two parameters ($k_\parallel$ and $k_\perp$ are conventionally used). This peculiarity of an $(n, 1)$ CNT is a consequence of its special crystal symmetry: the $(n, 1)$ CNT lattice can be obtained by translation of an elementary two-atom cell along a helical line on the nanotube wall (see Figure 2). As a result, the parameter k_s has the meaning of an electron wave vector along the helical line, and so any possible electron motion in an $(n, 1)$ CNT can be described by a de Broglie wave propagating along such a line. Both descriptions of the energy spectrum of an $(n, 1)$ CNT—by two parameters, $k_\parallel$ and $k_\perp$, or a single parameter k_s—are physically equivalent. However, the second description is more convenient for studies of electron processes determined by the above-mentioned helical symmetry of electron motion and allows one to discover new physical effects (e.g., the electron-electron interaction should be strongly modified for helical one-dimensional motion (Kibis, 1992)). We shall now show that such helical symmetry results in superlattice behavior of an $(n, 1)$ CNT in the presence of an electric field oriented perpendicular to the nanotube axis (a transverse electric field).

The potential energy of an electron on a helix subject to a transverse electric field is given by Eq. (1). In the case of a $(n, 1)$ CNT, the parameter R appearing in Eq. (1) corresponds to the radius of the nanotube, $R = C_h/2\pi$. The electron coordinate along the above-mentioned helical line is s, the length of a single coil of the helix l_0 is given by

$$l_0 = \frac{2\pi R}{\cos\theta} = \frac{2a(n^2 + n + 1)}{2n + 1}, \tag{17}$$

and the electric potential is assumed to be zero at the axis of the CNT. Since the period (17) of the electron potential energy is proportional to the CNT radius R and is greater than the interatomic distance $a_{C\text{-}C}$, the CNT assumes typical superlattice properties. It should be noted that an approach based on a superlattice analogy between different nanostructures has proven very productive in the theoretical treatment of low-dimensional systems. In particular, a similar approach was used by Yevtushenko et al. (1997), and Slepyan et al. (1998), in relation to nonlinear electronic transport in carbon nanotubes subjected to rapidly oscillating electric fields. Using the superlattice analogy for the case of an $(n, 1)$ CNT in a transverse electric field, one can predict that Bragg reflection of electron waves with wave vectors $k_s = \pm\pi/l_0$ results in energy splitting within the conduction and valence bands of the CNT. We shall now study this effect in more detail.

In the framework of the tight-binding model (see Saito, Dresselhaus, & Dresselhaus, 1998) considering only three nearest neighbors to each atom, the wave functions for electron states with corresponding energies (16) can be written as

$$\psi_j(k_s) = \frac{1}{\sqrt{2M}} \sum_t \left[\psi_t^{(A)} + (-1)^j \frac{h^*(k_s)}{|h(k_s)|}\psi_t^{(B)}\right] \exp(ik_s t a), \tag{18}$$

where M is the total number of two-atom cells in the CNT, $\psi_t^{(A)}$ and $\psi_t^{(B)}$ are π-orbital wave functions for the two carbon atoms A and B, respectively; t is the number along the helical line for an elementary cell consisting of these two atoms (see Figure 2); and $h(k_s) = 1 + \exp(-ik_s a) + \exp(ink_s a)$. The value of the potential energy U in the external electric field at the position of a particular atom of the CNT depends on the angle between the electric field vector and the vector normal to the nanotube axis which passes through this atom. As a consequence, the coordinate of atom A in cell number t along the helical line is

$$s = at + \frac{l_0}{2\pi}\phi. \tag{19}$$

The angle ϕ is defined such that $R\cos\left[\phi + \pi(n+1)/(n^2+n+1)\right]$ is the coordinate in the direction of the electric field (with zero at the CNT axis) of atom B in the cell with $t = 0$. Using Eqs. (18) and (19), we can write the matrix element of the potential energy (1) as

$$\langle\psi_i(k_s')|U|\psi_j(k_s)\rangle = V_{ij}^{+}\delta_{\cos(k_s a - k_s' a + 2\pi a/l_0),1} + V_{ij}^{-}\delta_{\cos(k_s a - k_s' a - 2\pi a/l_0),1}\,, \tag{20}$$

where

$$V_{ij}^{\pm} = \frac{eER}{4}\left[1 + (2\delta_{ij} - 1)\frac{h(k_s')h^*(k_s)}{|h(k_s')h(k_s)|}\exp\left(\pm i\frac{\pi(n+1)}{n^2+n+1}\right)\right]\exp(\pm i\phi) \tag{21}$$

and $\delta_{\alpha\beta}$ is the Kronecker delta. In the derivation of Eqs. (20) and (21) we have also assumed that the external electric field E is much less than the atomic field, i.e.,

$$E \ll \frac{\gamma_0}{ea}. \tag{22}$$

This allows us to neglect any change in the atomic wave functions $\psi_t^{(A)}$ and $\psi_t^{(B)}$ due to the field E, and we take into account only the mixing of states (18) by the field. According to Eq. (20), the field mixes only electron states (18) with wave vectors differing by $2\pi/l_0$. In this approximation, the exact wave function in the presence of the electric field, $\psi_E(k_s)$, can be expressed as a superposition of wave functions (18) with k_s shifted by integer numbers of $2\pi/l_0$:

$$\psi_E(k_s) = \sum_{j=1}^{2}\sum_{\nu=0}^{\mu-1} b_{j\nu}\psi_j\,(k_s + 2\pi\nu/l_0)\,. \tag{23}$$

To ensure that in Eq. (23) we sum only over *different* electron states, the parameter μ should be the smallest integer defined by the condition $\psi_j(k_s) = \psi_j\,(k_s + 2\pi\mu/l_0)$. This condition, together with the $2\pi/a$ periodicity of $\psi_j(k_s)$, implies that $\mu/l_0 = \beta/a$, where β is the smallest integer for which this equality is satisfied. Using Eq. (17) together with Eq. (10) one can obtain $\beta = (2n+1)/d_R$, which yields $\mu = N$. This result has a transparent physical interpretation, since the two closest carbon atoms equivalent with respect to a translation parallel to the nanotube axis are separated by a distance Na along a helical line.

Substituting the wave function (23) into the Schrödinger equation with the potential energy (1) we obtain a system of equations for the coefficients $b_{j\nu}$ entering Eq. (23):

$$\left[\varepsilon_j\left(k_s + 2\pi\nu/l_0\right) - \varepsilon_E(k_s)\right] b_{j\nu} + \sum_{i=1}^{2}\sum_{\nu'=0}^{N-1} \langle\psi_j\left(k_s + 2\pi\nu/l_0\right)|U|\psi_i\left(k_s + 2\pi\nu'/l_0\right)\rangle b_{i\nu'} = 0, \tag{24}$$

where $\nu = 0, 1, 2, \ldots, N-1$, the index j takes the value 1 or 2 for the valence and conduction bands, respectively, and $\varepsilon_E(k_s)$ is the electron energy in the presence of the transverse electric field.

Let us consider the states $k_s = -\pi/l_0$ and π/l_0 in the same CNT energy band, which are at the boundaries of a Brillouin zone created by the periodic "superlattice" potential (1) of the external field. One should expect the appearence of energy gaps at these values of k_s due to Bragg reflection of electron waves from the superlattice potential. These states are separated by $2\pi/l_0$ and have the same energy, which means that they are strongly mixed by the electric field. For these values of k_s it can be shown that the contributions to the sum in Eq. (23) from all other states can be neglected for sufficiently weak fields, $E \ll \gamma_0 a/(eR^2)$. As a result, the system of equations (24) is reduced to just two equations, from which the energy of Bragg band splitting $\Delta\varepsilon$ is found to be

$$\Delta\varepsilon = 2\left|\langle\psi_j(-\pi/l_0)|U|\psi_j(\pi/l_0)\rangle\right| \sim eER. \tag{25}$$

Thus, even a small electric field results in a superlattice-like change of the electron energy spectrum in $(n, 1)$ CNTs, with the appearance of Bragg energy gaps proportional to the field amplitude E and the nanotube radius R. Notably, this dependence of the Bragg gaps on the external field and radius applies to any helical quasi-one-dimensional nanostructure in a transverse electric field: this generic feature arises from the symmetry of the nanostructure, and is independent of the parameters of the tight-binding model used to derive Eq. (25). Indeed, this result coincides exactly with the Bragg energy gap (8) for nanohelices considered in the previous section.

It should be emphasized that the discussed superlattice behavior is a unique feature of $(n, 1)$ CNTs. For the general case of a (n, m) CNT with $m \neq 1$, the energy spectrum (15) depends on the quantum number l in addition to k_s. As already mentioned, l represents the projection of the electron angular momentum on the nanotube axis, and it follows from the corresponding selection rule that the transverse electric field only mixes electron states with angular momentum l and $l\pm1$. For $m \neq 1$, however, states with l differing by 1 correspond to different subbands, and in general have different energies for $k_s = \pm\pi/l_0$, so that there is no Bragg scattering between these states. The only effect of the electric field, therefore, is to mix electron states with different energies, which does not lead to noticeable modification of the dispersion curves for weak electric fields (Li, Rotkin, & Ravaioli, 2003).

For the particular case of a $(1, 1)$ CNT the energy spectrum can be obtained in analytic form for any electron state, since the system of equations (24) consists of four equations only. This system results in a biquadratic equation for the eigenvalues $\varepsilon_E(k_s)$:

$$\varepsilon_E^4(k_s) - \varepsilon_E^2(k_s)(w_1^2 + w_2^2 + 2v_1 + 2v_2) + (v_2 - v_1 + w_1 w_2)^2 = 0, \tag{26}$$

where $w_1 = \gamma_0[1 + 2\cos(k_s a)]$, $w_2 = \gamma_0[1 - 2\cos(k_s a)]$, $v_1 = [V\cos(\phi + \pi/3)]^2$, $v_2 = [\sqrt{3}V\sin(\phi+\pi/3)]^2$, and $V = \sqrt{3}eEa/(4\pi)$. The energy spectrum $\varepsilon_E(k_s)$ obtained from Eq. (26) is shown in Figure 3 (solid lines) for a range of wave vectors $-\pi/a \leq k_s \leq \pi/a$. In the figure, positive energies correspond to the conduction band and negative energies to the valence band. The energy spectrum in the absence of the field is shown for comparison (dashed lines). According to Eq. (17), the superlattice period l_0 for a (1, 1) CNT is equal to twice the lattice constant a. Therefore, as can be seen in Figure 3, the width of the first Brillouin zone in the presence of a transverse electric field is half that without the field. It can also be seen that the electric field opens gaps in the dispersion curve at $k_s = \pm\pi/(2a)$ due to the aforementioned Bragg reflection of electron waves. For electric fields satisfying condition (22), we obtain from Eq. (26) the Bragg gap

$$\Delta\varepsilon = \frac{\sqrt{3}eEa}{2\pi}|\cos(\phi + \pi/3)|. \tag{27}$$

The result in Eq. (27) can also be obtained from the more general formula (25). It should be noted that the Bragg gap, as well as the whole energy spectrum of the CNT in a transverse electric field, depends on the orientation of the CNT relative to the field (i.e., on the angle of rotation ϕ). In particular, when $\phi = \pi/6$ the Bragg gap (27) is zero: for this angle the values of the electric field potential at atoms A and B in a (1, 1)

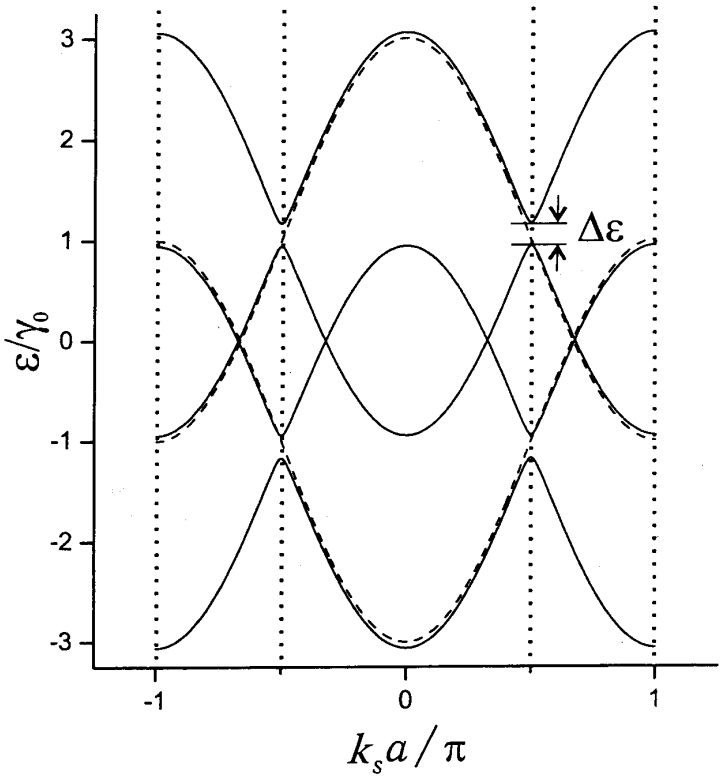

Figure 3. Electron energy spectrum of a (1, 1) CNT in the presence of a transverse electric field $E = \gamma_0/(ea_{C\text{-}C})$ with $\phi = 0$ (solid lines) and without the electric field (dashed lines). The inner pair of vertical dotted lines indicates the first Brillouin zone boundary in the presence of the field, whereas the outer pair corresponds to the first Brillouin zone boundary without the field. $\Delta\varepsilon$ is the Bragg gap opened by the electric field.

CNT are equal in magnitude but opposite in sign, and so the mean value of the potential within one elementary cell of the CNT is zero.

Figure 4 shows the results of the numerical energy spectra calculations for a (4, 1) CNT in a transverse electric field. Due to the superlattice effect discussed previously, the boundaries of the first Brillouin zone are now at $k_s = \pm\pi/(14a)$. One can see that even a small perturbation ($V = eER/4 = 0.1\gamma_0$) results in a significant modification of the electron spectra.

In the general case of an $(n, 1)$ nanotube, for external electric field intensities attainable in experiment ($E \sim 10^5$ V/cm) and for a typical nanotube of radius $R \sim 10$ Å, the value of the Bragg gap given by (25) is $\Delta\varepsilon \sim 10^{-2}$ eV, which is comparable to the characteristic energy of band splitting in conventional semiconductor superlattices. As a consequence, the discussed superlattice effects generated by the transverse electric field in $(n, 1)$ CNTs should be observable in experiments and may take place in existing CNT field-effect devices (Appenzeller et al., 2002). The inherent regularity of a nanotube-based superlattice, with the superlattice period determined by the CNT radius, presents a distinct advantage over semiconductor superlattices, in which monolayer fluctuations are unavoidable. A whole range of new nanoelectronic devices based on the discussed superlattice properties of $(n, 1)$ CNTs can be envisaged, including Bloch oscillators (Esaki & Tsu, 1970) and quantum cascade lasers (Faist et al., 1994). An evaluation of the feasibility of these novel devices and selection of their optimal parameters will undoubtedly form the subject of extensive future research.

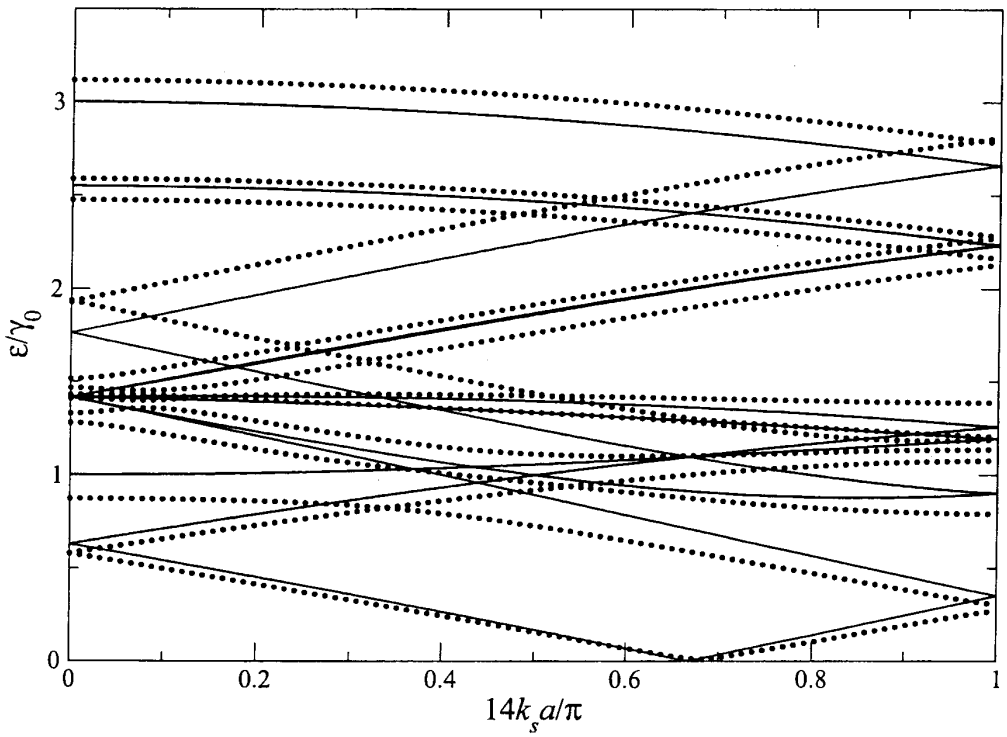

Figure 4. Electron energy spectrum (positive energies only) of a (4, 1) carbon nanotube in the presence of a transverse electric field $E = 0.4\gamma_0/(eR)$ (circles) and in the vanishing field (solid lines). Note that $\varepsilon(-k_s) = \varepsilon(k_s)$, and that the negative energy values can be obtained by the mirror reflection of the graph in the horizontal ($\varepsilon = 0$) axis.

Conclusions

In this paper we have discussed a previously overlooked class of CNTs, which may be termed "helical" nanotubes. While we have concentrated on the superlattice behavior of such nanotubes in a transverse electric field, we also expect their unique symmetry to manifest itself in modification of the electron–electron, electron–phonon, and electron–photon interactions. In addition, we have shown that superlattice behavior in a transverse electric field is a generic feature of helical quasi-one-dimensional nanostructures, which raises new possibilities for developing optoelectronic devices operating in the terahertz range of frequencies.

References

Appenzeller, J., J. Knoch, V. Derycke, R. Martel, S. Wind, & Ph. Avouris. 2002. Field-modulated carrier transport in carbon nanotube transistors. *Phys. Rev. Lett.* 89:126801.

Esaki, L., & R. Tsu. 1970. Superlattice and negative differential conductivity in semiconductors. *IBM J. Res. Dev.* 14:61–65.

Faist, J., F. Capasso, D. L. Sivco, C. Sirtori, A. L. Hutchinson, & A. Y. Cho. 1994. Quantum cascade laser. *Science* 264:553–556.

Gradshteyn, I. S., & I. M. Ryzhik. 2000. *Table of integrals, series, and products*. San Diego: Academic Press.

Iijima, S. 1991. Helical microtubules of graphite carbon. *Nature* 354:56–58.

Ivchenko, E. L., & G. E. Pikus. 1997. *Superlattices and other heterostructures*. Berlin: Springer-Verlag.

Kibis, O. V. 1992. Electron-electron interaction in a spiral quantum wire. *Phys. Lett. A* 166:393–394.

Kibis, O. V., D. G. W. Parfitt, & M. E. Portnoi. 2005. Superlattice properties of carbon nanotubes in a transverse electric field. *Phys. Rev. B* 71:035411.

Li, Y., S. V. Rotkin, & U. Ravaioli. 2003. Electronic response and bandstructure modulation of carbon nanotubes in a transverse electrical field. *Nano Lett.* 3:183–187.

Prinz, V. Ya., V. A. Seleznev, A. K. Gutakovsky, A. V. Chehovsky, V. V. Preobrazhenskii, M. A. Putiato, & T. A. Gavrilova. 2000. Free-standing and overgrown InGaAs/GaAs nanotubes, nanohelices and their arrays. *Physica E* 6:828–831.

Prinz, V. Ya., D. Grützmacher, A. Beyer, C. David, B. Ketterer, & E. Deckardt. 2001. A new technique for fabricating three-dimensional micro- and nanostructures of various shapes. *Nanotechnology* 12:399–402.

Saito R., G. Dresselhaus, & M. S. Dresselhaus. 1998. *Physical properties of carbon nanotubes*. London: Imperial College Press.

Slepyan, G. Ya., S. Maksimenko, A. Lakhtakia, O. M. Yevtushenko, & A. V. Gusakov. 1998. Electronic and electromagnetic properties of nanotubes. *Phys. Rev. B* 57:9485–9497.

Yevtushenko, O. M., G. Ya. Slepyan, S. Maksimenko, A. Lakhtakia, & D. A. Romanov. 1997. Nonlinear electron transport effects in a chiral carbon nanotube. *Phys. Rev. Lett.* 79:1102–1105.